THE BALTIC JOURNAL
OF ROAD AND BRIDGE ENGINEERING
2026/21(2)

ISSN 1822-427X/eISSN 1822-4288
2026 Volume 21 Issue 2: 61–88
https://doi.org/10.7250/bjrbe.2026-21.678

AN EXAMPLE OF ROAD DETERIORATION AND STABILIZATION SOLUTIONS WITH BORED PILE: LOCAL LANDSLIDE TRIGGERED BY GYPSUM KARST ON THE ULUYAZI CAMPUS ROAD (ÇANKIRI, TÜRKİYE)

ÇIĞDEM YETİŞ GÖREN[1], ENDER SARIFAKIOGLU[1,*], ADEN-GANI ROBLEH SAMIREH[1], BAŞAK VARLİ BİNGÖL[1], JURIS BURLAKOVS[2]

[1] *Civil Engineering Department, Çankırı Karatekin University, Çankırı, Türkiye*

[2] *Civil Engineering Department, Riga Technical University, Riga, Latvia*

Received 24 January 2026; accepted 6 March 2026

Abstract. A localized landslide that occurred on a specific section of the road to the Uluyazı Campus of Çankırı Karatekin University seriously threatened road safety and disrupted transportation continuity. In this study, the ground conditions of the landslide area were examined in detail. Soil parameters were determined through field observations, drilling, Standard Penetration Test (SPT) data, laboratory experiments, liquefaction potential, bearing capacity, and consolidation behaviour were analysed. The analyses showed that the soil was safe in terms of liquefaction and that the bearing capacity was at a level suitable for road construction and use. However, consolidation settlements and dissolutions in gypsum levels were identified as critical factors that could trigger landslides. To prevent landslides

* Corresponding author. E-mail: enders@karatekin.edu.tr

Çiğdem YETİŞ GÖREN (ORCID ID 0000-0002-9749-606X)
Ender SARIFAKIOGLU (ORCID ID 0000-0001-6930-000X)
Aden-gani ROBLEH SAMIREH (ORCID ID 0009-0007-6584-8407)
Varli BİNGÖL (ORCID ID 0000-0002-7934-7482)
Juris BURLAKOVS (ORCID ID 0000-0003-0269-4790)

and ensure road safety, double rows of bored piles with a diameter of Ø120 cm, a length of 35 m, and spaced at 1.4 m intervals were connected with a cap beam. This engineering measure cut the landslide surface, limited road deformations, and ensured transportation safety. The study demonstrated the effectiveness of bored pile applications in formations where soil-water interaction was significant and offered an applicable solution for critical areas in highway engineering.

Keywords: bored piles, bearing capacity, consolidation, landslide, liquefaction potential, road safety, soil-water interaction.

Introduction

Landslides, one of the natural disasters commonly observed worldwide, are defined as the downward or outward movement and displacement of natural rock, soil, or artificial fill materials, or their mixture on a slope (Terzaghi, 1950; Varnes, 1958, Cruden, 1991; USGS, 2008). Factors such as climatic conditions (heavy rainfall), groundwater levels, landforms (especially, steep slopes), lithological characteristics (especially, the presence of clay layers), and human activities (such as road, tunnel, and dam construction) cause soil movement and displacement (ÇEM, 2016). Landslides pose serious socio-economic impacts, leading to loss of life, and damage to roads, railways, agricultural areas, and residential buildings, and damage and loss of cultural and natural heritage. In Türkiye, some devastating landslides were reported (Ocakoğlu et al., 2002). In the Black Sea and Mediterranean regions, small and large-scale landslides and rockfalls occur every year following periods of heavy rainfall. The geographical, morphological, geological, and groundwater factors of the region are prominent in triggering these sliding mechanisms. In the region located in the transition zone between Central Anatolia and the Eastern Black Sea (Koyulhisar, Sivas), a landslide occurred in March (2005), primarily consisting of debris and mud flowing rapidly onto the settlement area within the valley, resulting in the deaths of 15 people. One of the most important factors that prepared and accelerated this landslide was the surface and groundwater seeping from melting snow, utilising the intense discontinuities and normal fault planes observed in and around the crown region. This water oversaturated the highly altered volcanic rocks, causing the movement of material, mostly derived from volcanic rocks, along a failure surface that developed between the underlying limestone and the altered volcanic rocks (Gürsoy et al., 2024). Avşar et al. (2014) investigated the Aksu landslide on the Giresun-Espiye road in the Eastern Black Sea Region. Weathered tuff, flysch, and dacitic tuffs are common in the study area. Excavations at the foot of the slope (i.e., due to the foundation excavation for the tunnel restaurant building and road construction) caused a “translational slide”. The stability of the slope containing weathered tuff was disrupted, and the rise in the groundwater level also contributed to the landslide. However, heavy rainfall in the Eastern Black Sea Region is causing floods and landslides in settlements. In particular, the Dereli district of Giresun has been filled with mud, stones, rubble, and tree fragments reaching up to 3 meters in depth. This disaster has resulted in the deaths of dozens of people and significant economic losses (Kömürçü et al., 2021). When estimating the landslide susceptibility of the region, the following parameters were used to provide preliminary probability expectations regarding the likelihood of occurrence: geology, elevation, slope, aspect, curvature (plan and profile curvature), soil depth, topographic moisture index, land cover, and proximity to roads and streams (Gokceoglu & Aksoy, 1996; Yalcin & Bulut, 2007; Akıncı et al., 2014).

In Türkiye, particularly in claystone and mudstone formations containing gypsum levels, sliding mechanisms are easily triggered by surface and groundwater effects. Gypsum outcrops are generally located in Central Anatolia (Doğan, 2002; Waltham, 2002; Ateş et al., 2008). Due to its interaction with water, gypsum karst areas form karst cavities that are similar to limestone. Gypsum has a higher solubility than limestone (Cooper & Gutiérrez, 2013; Doğan & Yeşilyurt, 2019). Therefore, collapse sinkholes commonly develop in fine-grained soils containing gypsum levels. The landslides caused by these gypsum sinkholes have caused so much damage that they have resulted in the displacement of settlements in Central Anatolia (i.e., İnandık Village in Çankırı province) (Özçelik et al., 2016; Gökkaya & Tunçel, 2019; Yıldız & Sarıfakıoğlu, 2022).

Also, this situation poses serious risks for transportation systems such as roads, bridges, and infrastructure. Landslides create serious hazards, especially in critical transportation infrastructure such as highways. These effects can be classified primarily as follows (Erginal & Bayrakdar, 2005; KGM, 2022; Tırın, 2023):

- Structural damage risk: Landslide debris flowing onto the road can cause cracks, deformations, and subsidence in the asphalt and fill material. This situation can lead to loss of control by drivers and vehicle damage.
- Traffic safety: Sudden or slow-moving landslides can cause road narrowing, sudden obstacles, and reduced visibility. These risks increase especially at night or in rainy weather.
- Infrastructure and Service Disruption: Landslides can clog drainage lines along the road, strain bridges and culverts, and increase the risk of flooding. This can cause disruption to emergency and logistical services.
- Continuous maintenance and cost: Roads in landslide-prone areas require constant monitoring, repair, and reinforcement. This creates both cost and operational challenges.

In this context, landslide observations on the Uluyazı Campus road are important not only as a geotechnical issue but also in terms of sustainable road safety planning. In areas where landslide risk has been identified, ground stability can be ensured and road safety enhanced through the use of pile foundations, slope stabilization, and effective drainage systems. In this context, the Uluyazı (Çankırı) Campus road provides a typical field example. Cracks, deformations, and fissures developing along the slope observed along the road route indicated a local landslide event in the ground. In this study, the development mechanism of the landslide in question was revealed using geological, geotechnical, and hydrogeological data; the bored pile solution applied in the field was evaluated from a technical perspective.

1. Geology of the study area

The study area is located in the Uluyazı region of Çankırı province, approximately 40 km south of the North Anatolian Fault Zone (Ketin, 1976). This location places the region within an active tectonic belt (Figure 1). The lithology of the region is generally represented by units belonging to the Bozkır formation (Sarıfakıoğlu et al., 2011; Sarifakioglu et al., 2021). The formation consists of alternating layers of claystone and silty sandstone. Within this alternation, there are mostly gypsum levels of varying thickness. Other rock units are found in the Bayındır and Kızılırmak formations. Bayındır formation consists of alternating layers of sandstone, mudstone and partly gypsium levels while The Kızılırmak formation mainly contains red mudstone and occasionally gypsum thin interlayers. The Bayındır and Bozkır formations reflect evaporitic conditions in a closed lake environment (Sevin & Uğuz, 2011). The Değim formation is encountered in a limited area. The unit, which presents alluvial fan conditions, consists of maroon, brown, and yellowish conglomerate, minor amounts of sandstone, and mudstone (Figure 2).

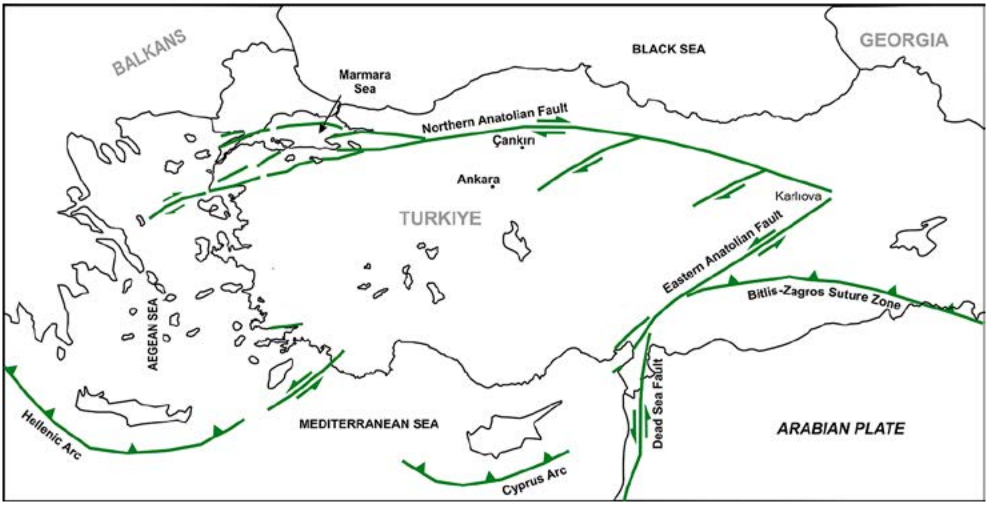

Figure 1. The location of Çankırı, where the study area is located (simplified from MTA, 2001)

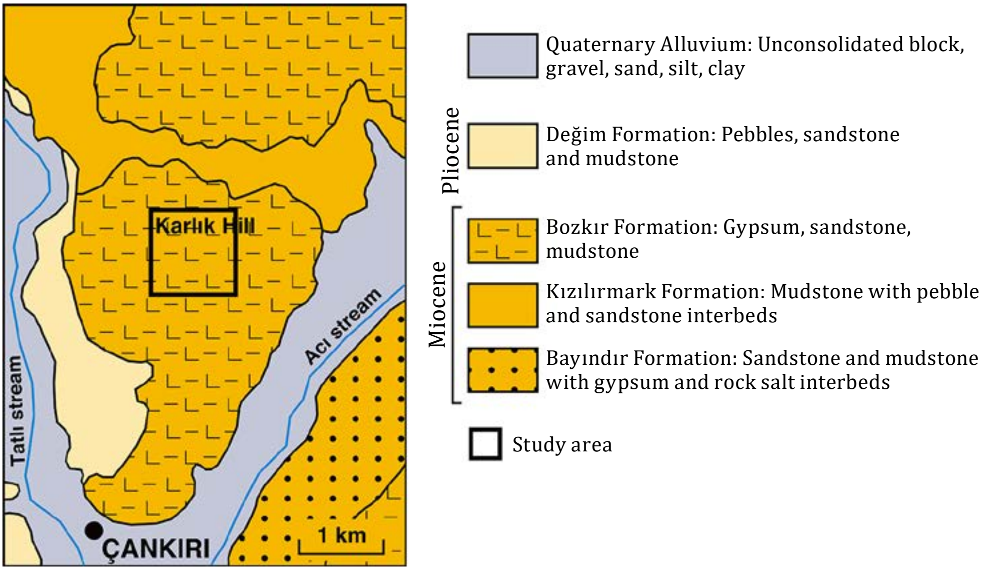

Figure 2. Geological map of the study area (taken from Sevin & Uğuz, 2011)

Fine-grained sedimentary rocks of the Bozkır formation such as claystone and mudstone are notable for their low permeability and high plasticity values. When saturated with water, these types of soils rapidly lose their shear strength and become extremely conducive to the development of a slip surface. Sandstone layers, while relatively more resistant, do not play a significant role in inhibiting landslide behaviour due to their discontinuities. Landslide areas are marked in Figure 3.

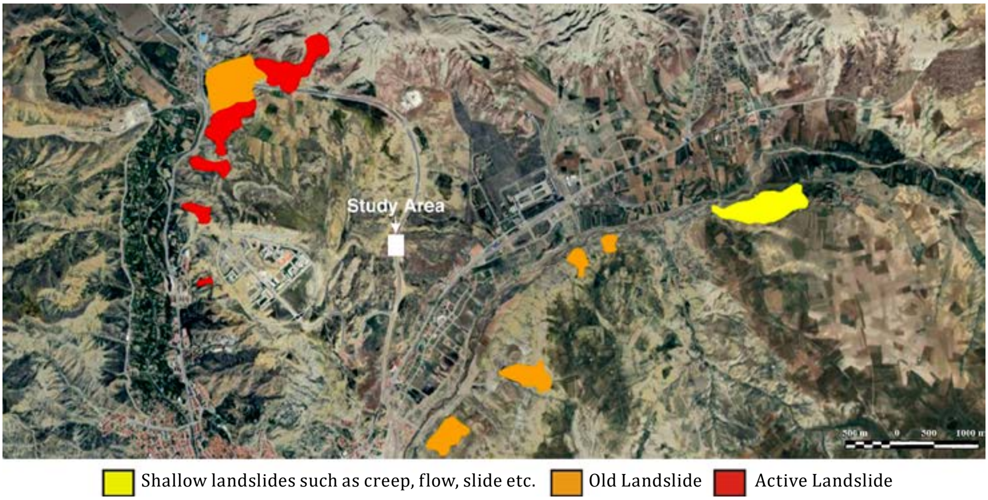

Figure 3. Landslide areas around Çankırı Karatekin University, Uluyazı Campus

Gypsum levels are the most critical lithological component of the region from an engineering perspective. Gypsum is a mineral that dissolves easily when it comes into contact with water. Therefore, contact between groundwater and rainwater and gypsum layers leads to the development of dissolution voids over time. Dissolution voids disrupt the homogeneity of the ground, reduce its bearing capacity, and cause sudden settlements and local stability losses. This process poses significant risks, especially in the subgrade where road embankments are located. Field observations revealed that different settlements developed under the road embankment, causing cracks and fissures to form on the surface. Examination of the sinkholes revealed that the fill material used in the road subgrade consisted of gypsum blocks taken from the road cut. In addition, the aggregate sizes used in the cross-section area of the road superstructure were also observed (Figure 4).

Figure 4. (a, b) Gypsum block filling material of the road infrastructure in the collapse pits and aggregates used in the road superstructure

Groundwater levels measured during drilling in the study area were recorded at depths of 5.0–6.5 m. Seasonal variations in groundwater levels were observed: levels rise during the rainy spring and winter months and recede to relatively deeper levels during the summer months. This seasonal fluctuation causes periodic increases in pore water pressure and temporary losses in soil strength. Increased contact with gypsum layers, especially during rainy periods, accelerates dissolution processes and poses an engineering risk.

In Çankırı and its surroundings, the most important formation carrying sufficient groundwater for irrigation, industry, and drinking water is the clayey, sandy, and gravelly alluvium extending along the Tatlıçay, Acıçay, and Eldivan Çayı rivers. The thickness of the alluvium varies between 10–35 m. Volcanic rocks found at high elevations in the region carry a small amount of groundwater. Numerous small springs (with a discharge of less than 51 sec) emerge from the volcanic rocks. Ophiolites and red-colored formations of Oligocene-Miocene age do not carry sufficient groundwater. Gypsum deposits located in the relatively low-lying areas of the region are unfavourable in terms of groundwater due to salinity (Çankırı Governorship, 2023).

The geomorphological characteristics of the site also facilitate landslide development. The section where the campus road passes extends along a slope with a relatively steep gradient. Cracks and fissures observed along the slope allow surface water to easily seep into the ground. Due to inadequate surface water drainage, rainwater accumulates on the slope body, increasing pore water pressure and accelerating stability loss on the sliding surface.

Çankırı Karatekin University, along the Uluyazı campus road, features loose soil characteristics with thin gypsum layers observed in places, consisting of greyish sandy and/or clayey silt (red mudstone) lithological units. Studies have been conducted to investigate a landslide that occurred in a local area along the campus road. The landslide caused subsidence and cracks/fissures in the road surface and deformations in the surrounding area (Figure 5). The subsidence pits grew over time, posing a risk to the road route.

Figure 5. (a, b) Collapse and cracks-fissures on the Uluyazı campus road surface; (c, d) collapse pits

2. Materials and methods

In the vicinity of the Uluyazı Campus, the relevant company conducted a total of 60.00 m of drilling work at 3 different locations for landslide studies, and 27 SPT (Standard Penetration Test, disturbed sample) and 1 UD (undisturbed sample) samples were taken. The boreholes were drilled with diameters of 75 mm and 76 mm. Summary information on the drilling is presented in Table 1.

Table 1. Characteristics of the drilling wells conducted in the field

Drilling No.	Coordinate (UTM 3-ED 50°-DN:33)		*Z*, m	Depth, m	SPT, piece	UD, piece
	X	*Y*				
HSK-1	4499401	553845	825	20.00	8	1
HSK-2	4499333	553842	821	20.00	11	1
HSK-3	4499367	553841	823	20.00	8	
			Total	60	27	2

SPT is an in-situ test and one of the most frequently used and oldest field tests in soil investigations. The blow counts obtained in this test are values determined in the undisturbed state of the soil. The penetration resistance of the soil is expressed as the number of blows required to drive a 63.5 kg standard tube, dropped freely from a height of 76 cm, into the soil to a depth of 30 cm. SPT (disturbed sample) selected to represent the drilling carried out in silty clay soils in the investigation area, UD (undisturbed sample), and core samples were taken for laboratory testing. The data obtained from the drilling works were evaluated according to ISO 22475-1:2006 for groundwater measurements, ASTM D1586 for SPTs, and ASTM D1587 for UDs.

2.1. Analysis of SPT values

The necessary adjustments have been made to the number of blows (N) applied to achieve the second and third 15 cm advances. These adjustments were made taking into account various factors such as variability in the soil profile, equipment differences, and energy transfer efficiency. The resulting corrected blow count is expressed as the standardized $N_{1.60}$ value. This value, $N_{1.60}$, is critical for the reliable interpretation of SPT results. In particular, it is used directly in soil bearing capacity calculations, settlement analyses, and the evaluation of liquefaction potential.

$$N_{1.60} = N \times C_{\mathrm{E}} \times C_{\mathrm{N}} \times C_{\mathrm{B}} \times C_{\mathrm{S}} \times C_{\mathrm{R}}. \tag{1}$$

The depth correction factor (CN) used to enhance the reliability of SPT results is only considered for cohesionless soils (such as sand and gravel). In cohesive (clay) soils, the application of this coefficient is not appropriate due to undrained behaviour. Based on the formula proposed by Liao and Whitman (1986), the CN coefficient is determined using the vertical effective stress (σ'_{vi}) calculated in the layer related to atmospheric pressure (Pa).

Effective stress (σ'_{vi}) is calculated by subtracting pore water pressure (u) from total vertical stress (σ_{vi}). The total vertical stress is calculated as the product of the depth of the layer centre to the ground surface (z) and the saturated unit weight (γ_s). The unit weight of water (γ_w = 9.81 kN/m^3) is taken into account when determining the pore water pressure.

2.2. Calculation of liquefaction potential

Liquefaction that can occur under earthquake loads can cause serious problems not only in building foundations but also in road pavements. In soils that lose their bearing capacity due to liquefaction, the roadbed suddenly settles, undulates, and the pavement layer deteriorates. This situation, which is particularly common in sandy soils, both reduces road safety and increases maintenance and repair costs. Therefore, accurately assessing the potential for liquefaction is also a critical requirement for the sustainability of road infrastructure in earthquake-prone areas.

In this study, blow counts obtained from SPT tests were used to determine the liquefaction potential of soils. The analysis was based on the Simplified Procedure, which was developed based on field data and is widely used in engineering applications. This approach, first proposed by Youd & Noble (1997), was later developed and updated by Youd et al. (2001). Liquefaction safety is evaluated by comparing the soil's resistance capacity (*CRR* – cyclic resistance ratio) with the shear stress demand (*CSR* – cyclic stress ratio) generated during an earthquake, using the Safety Factor (*FS*). It is calculated as shown in Equation (2).

$$FS = \frac{CRR}{CSR} \times MSF \tag{2}$$

Here, $FS > 1.0$ indicates that the soil is safe against liquefaction, while $FS < 1.0$ indicates a risk of liquefaction. The method is widely preferred in field studies because it provides reliable results, especially in sandy soils.

The *CRR* value, which represents the soil's resistance, was calculated using empirical relationships proposed by Youd et al. (2001). The $N_{1.60\mathrm{f}}$ parameter used in these relationships was obtained by adding the effect of the fine particle ratio to the standard $N_{1.60}$ value. The fine-grained correction was made by using different coefficients depending on the effect of the fine-grained ratio. However, since soils with $N_{1.60f} \geq 30$ are generally considered very dense and impermeable, such layers are considered safe in terms of liquefaction according to the literature.

The repeated stress ratio (CSR) formed in the ground during an earthquake is calculated using the empirical relationship developed by Seed and Idriss (1971). This equation takes into account the maximum horizontal acceleration at the surface ($a_{\max}$), the vertical effective stress ratio (σ_{vi}/σ'_{vi}), and the stress reduction factor (r_d), which varies with depth. The values of the coefficient r_d are based on the depth-dependent equations proposed by Liao & Whitman (1986).

Additionally, the magnitude-dependent correction factor (MSF) was calculated using the formula provided by Idriss (1995). In this study, the design earthquake magnitude was taken as $M_w = 6.0$, and the Turkey Earthquake Hazard Map (AFAD, 2019) was used as a reference in the analyses.

2.3. Seating analysis

One of the most important geotechnical parameters in terms of structural safety is settlement behaviour. Soil layers deform under applied loads, leading to settlement over time. This settlement consists of different processes, namely instantaneous elastic deformation, consolidation settlement, and secondary settlement (Das & Sobhan, 2013). Factors such as soil type, depth of groundwater level, and loading duration are taken into account in calculations. Terzaghi's Consolidation Theory is widely used to determine consolidation settlements, especially in cohesive (clayey) soils (Craig, 2004). Different settlements occurring under flexible pavements cause wheel ruts to form on the surface over time and lead to the development of longitudinal and transverse cracks. In particular, the prolonged consolidation process in clayey soils causes irregular deformations in the road pavement. This situation reduces vehicle comfort, negatively affects road safety, and increases maintenance frequency. Therefore, settlement analyses must also be addressed in detail.

2.4. Load-bearing capacity analysis

Soil bearing capacity analysis is a fundamental geotechnical assessment that examines whether the loads imposed on foundations can be safely supported. During this analysis, the final bearing capacity is calculated by considering the soil type, groundwater level, foundation geometry, and loading conditions. Stroud (1974) established a correlation between the undrained shear strength (cu) of the soil and its bearing capacity using laboratory tests and SPT results, and developed reliable calculation methods, particularly for low-strength soft soils. Roads built on soils with insufficient bearing capacity exhibit cracking, shear failures, and settlement problems in the pavement layer, especially under heavy vehicle traffic. Such failures shorten the service life of the road and increase maintenance costs.

2.5. Determination of undrained shear strength

The undrained shear strength of cohesive soils is calculated using the relationships proposed by Stroud (1974), taking into account the SPT blow count (N) and the plasticity index (PI). In this approach, the undrained shear strength of soil units is determined using coefficients (f_1) dependent on the plasticity index.

2.6. Ultimate and safe bearing capacity

The concepts of ultimate bearing capacity (q_f) and safe bearing capacity (q_s) are used in determining the bearing capacity of soils. The ultimate bearing capacity is calculated using the equation provided by Craig (2004), based on the relationships proposed by Skempton (1951). The safe bearing capacity is obtained by taking into account the safety factor (GS) (Uzuner and Özmen, 1991).

$$q_\mathrm{f} = 5.14cu, \tag{3}$$

where GS is generally selected between 2 and 5 depending on ground conditions and engineering practice, and in most cases, 3 is taken.

3. Findings and discussion

In the vicinity of the Uluyazı Campus, SPT borehole studies conducted at three different locations by the relevant company for landslide studies revealed that the groundwater level varied between 5 m and 6.5 m. In the project area, groundwater levels were accepted at the surface to simplify mathematical calculations during the settlement analysis. The soil drilling profile consists of approximately 1.5 meters of road fill and, generally up to a depth of approximately 20 meters, mainly dark brown-reddish coloured claystone and/or silty claystone (mudstone) containing thin gypsum interlayers in places, with very little loosely cemented. It was determined that the lithological characteristics observed in the field corresponded to the lithological characteristics of the samples taken from the drilling wells (Figures 6, 7). Atterberg limit tests conducted on undisturbed samples taken from boreholes resulted in plasticity indices (PI) of 30.7%, 23.7%, and 16.5%. These results indicate that the soil exhibits medium-high plasticity clay characteristics, and settlement and swelling potential must be taken into account. In particular, the presence of thin gypsum interlayers may cause local weaknesses and heterogeneity in soil behaviour, necessitating the cautious selection of safety factors in engineering designs.

Furthermore, assuming the groundwater level to be close to the surface has led to drainage conditions and effective stress distributions playing a more critical role in the analyses.

Figure 6. The area where the drilling well is located, silty sandstone (sst), gypsum levels and dark brown-reddish mudstones (mst)

Figure 7. The SPT used in the area located in the dark brown-reddish mudstones (mst) and thin-grain sandstones (sst) containing gypsum (gps) layers

3.1. Atterberg limit test

Atterberg limit tests conducted on undisturbed samples taken from the project area revealed a plasticity index (PI) of 30.7% at a depth of 1.50 m from the surface in borehole HSK-1; in SK-2 borehole, the plasticity index (PI) at a depth of 1.50 m from the surface was determined to be 23.7%, and in SK-3 borehole, the plasticity index (PI) at a depth of 1.50 m from the surface was determined to be 16.5%. The soil class in the study area is mostly high plasticity clay (CH), with some sandy clay (SC) characteristics. These soil properties are critical in road fill and subgrade design. In particular, since highly plastic clay layers may exhibit swelling and settlement behaviour when in contact with water, effective drainage measures and mechanically improved fill materials should be applied to ensure the long-term stability of the road base. To minimise the potential impact of clay layers with high plasticity indices on road safety, the slope angle, fill density, and soil improvement methods should be carefully planned for slopes and fill edges.

3.2. SPT values

The methods defined by Robertson & Wride (1998) and Youd et al. (2001) were used to correct the SPT results (Tables 2–4). Consolidation settlement is expected in all silt and clay soils with *N* values less than 30, which are very soft, soft, medium stiff, stiff, and very stiff.

Table 2. SPT correction for HSK-1 Borehole

Depth, m	Soil Class	*N*	σ_{v0}, kN/m²	σ'_{v0}, kN/m²	C_N	C_E	C_B	C_R	C_S	N_{60}
1.50–1.95	CH	36	31.81	31.81	1.00	1.00	1.00	0.75	1.00	12
3.00–3.45	CH	12	59.47	59.47	1.00	1.00	1.00	0.80	1.00	9.6
4.50–4.95	Insufficient	13	87.13	87.13	1.00	1.00	1.00	0.85	1.00	11.05
6.00–6.45	CH	38	114.79	112.58	0.93	1.00	1.00	0.95	1.00	33.57
7.50–7.95	CH	43	142.45	125.53	0.89	1.00	1.00	0.95	1.00	36.36
9.00–9.45	CH	47	170.11	138.47	0.85	1.00	1.00	0.95	1.00	37.95
10.50–10.95	CH	57	197.77	151.42	0.81	1.00	1.00	1.00	1.00	46.17
12.00–12.21	CH	R	223.22	163.33	0.78	1.00	1.00	1.00	1.00	≥50

Depth, m	α	β	$N_{1.60CS}$	a_{max}	r_d	M_w	*CRR*	*CSR*	*MSF*	*FS*
1.50–1.95	2.77	1.05	31.12	0.3	0.99	6	0.57	0.193	1.77	5.23
3.00–3.45	5	1.2	16.52	0.3	0.97	6	0.18	0.189	1.77	1.69
4.50–4.95	5	1.2	18.26	0.3	0.96	6	0.19	0.187	1.77	3.97
6.00–6.45	5	1.2	45.28	0.3	0.95	6	0.24	0.189	1.77	2.25
7.50–7.95	5	1.2	48.63	0.3	0.94	6	0.29	0.208	1.77	2.47
9.00–9.45	5	1.2	50.54	0.3	0.92	6	0.31	0.264	1.77	2.08
10.50–10.95	5	1.2	60.40	0.3	0.88	6	0.41	0.278	1.77	2.61
12.00–12.21	5	1.2	-	0.3	0.85	6	-	-	1.77	-

Table 3. SPT correction for HSK-2 Borehole

Depth, m	Soil Class	N	σ_{vi}, kN/m²	σ'_{vi}, kN/m²	C_N	C_E	C_B	C_R	C_S	N_{60}
1.50–1.95	CH	27	31.81	31.81	1.00	1.00	1.00	0.75	1.00	20.25
3.00–3.45	CH	12	59.47	59.47	1.00	1.00	1.00	0.80	1.00	9.6
4.50–4.95	CH	20	87.13	87.13	1.00	1.00	1.00	0.85	1.00	17.0
6.00–6.45	CH	18	114.79	107.68	0.96	1.00	1.00	0.95	1.00	16.4
7.50–7.95	CH	43	142.45	120.62	0.91	1.00	1.00	0.95	1.00	37.2
9.00–9.45	CH	51	170.11	133.57	0.87	1.00	1.00	0.95	1.00	42.2
10.50–10.95	CH	50	197.78	146.51	0.83	1.00	1.00	1.00	1.00	41.5
12.00–12.45	CH	R	225.43	159.46	0.79	1.00	1.00	1.00	1.00	≥50
13.50–13.8	CH	R	251.71	171.75	0.76	1.00	1.00	1.00	1.00	≥50
15.00–15.1	NO	R	277.52	183.84	0.74	1.00	1.00	1.00	1.00	-
16.50–16.5	NO	R	304.26	196.35	0.71	1.00	1.00	1.00	1.00	-

Depth, m	$N_{1.60}$	α	β	$N_{1.60CS}$	a_{max}	r_d	M_w	*CRR*	*CSR*	*MSF*	*FS*
1.50–1.95	20.25	5	1.2	29.3	0.3	0.99	6	0.43	0.193	1.77	3.94
3.00–3.45	9.6	5	1.2	16.52	0.3	0.97	6	0.18	0.189	1.77	1.68
4.50–4.95	17.0	5	1.2	25.4	0.3	0.96	6	0.30	0.187	1.77	2.84
6.00–6.45	16.4	5	1.2	24.68	0.3	0.95	6	0.29	0.197	1.77	2.61
7.50–7.95	37.2	5	1.2	49.64	0.3	0.94	6	0.30	0.216	1.77	2.46
9.00–9.45	42.2	5	1.2	55.64	0.3	0.92	6	0.36	0.228	1.77	2.79
10.50–10.95	41.5	5	1.2	54.8	0.3	0.88	6	0.39	0.231	1.77	2.99
12.00–12.45	≥50	5	1.2	-	0.3	0.84	6	-	0.232	1.77	-
13.50–13.8	≥50	5	1.2	-	0.3	0.81	6	-	0.231	1.77	-
15.00–15.1	-	5	1.2	-	0.3	0.77	6	-	0.227	1.77	-
16.50–16.5	-	5	1.2	-	0.3	0.73	6	-	0.221	1.77	-

Table 4. SPT correction for HSK-3 Borehole

Depth, m	Soil Class	N	σ_{vi}, kN/m²	σ'_{vi}, kN/m²	C_N	C_E	C_B	C_R	C_S	N_{60}
1.50–1.95	SC	14	31.81	31.81	1.00	1.00	1.00	0.75	1.00	10.5
3.00–3.45	SC	21	59.47	59.47	1.00	1.00	1.00	0.80	1.00	16.8
4.50–4.54	CH	R	83.35	83.35	1.00	1.00	1.00	0.85	1.00	R
6.00–6.45	CH	16	114.79	102.77	0.99	1.00	1.00	0.95	1.00	15.0
7.50–7.95	CH	42	142.45	115.72	0.93	1.00	1.00	0.95	1.00	37.1
9.00–9.45	CH	54	170.11	128.66	0.88	1.00	1.00	0.95	1.00	45.1
10.50–10.95	CH	60	197.78	141.61	0.84	1.00	1.00	1.00	1.00	50.4
12.00–12.45	CH	56	225.43	154.55	0.80	1.00	1.00	1.00	1.00	44.8
Depth, m	α	β	$N_{1.60CS}$	a_{max}	r_d	M_w	*CRR*	*CSR*	*MSF*	*FS*
1.50–1.95	2.14	1.04	13.08	0.3	0.99	6	0.41	0.193	1.77	3.76
3.00–3.45	2.99	1.05	20.63	0.3	0.97	6	0.22	0.189	1.77	2.06
4.50–4.54	5	1.2	-	0.3	0.96	6	-	0.187	1.77	-
6.00–6.45	5	1.2	23	0.3	0.95	6	0.26	0.206	1.77	2.23
7.50–7.95	5	1.2	49.52	0.3	0.94	6	0.30	0.226	1.77	2.35
9.00–9.45	5	1.2	59.12	0.3	0.92	6	0.39	0.237	1.77	2.91
10.50–10.95	5	1.2	65.48	0.3	0.88	6	0.45	0.240	1.77	3.32
12.00–12.45	5	1.2	58.76	0.3	0.84	6	0.39	0.239	1.77	2.89

This value corresponds to the soil class “medium tight-tight” for clayey/clayey sandy soils according to the soil classification of Terzagi & Peck (1967) and Clayton (1993).

3.3. Potential for liquefaction

Soil liquefaction is an event that occurs in some water-saturated soils during earthquakes and causes significant surface deformations. It is particularly observed in alluvial soils where the groundwater level is shallow and the soil type exhibits loose characteristics. The North Anatolian Fault Zone, located in the north of Çankırı province, is an important seismic source capable of producing large earthquakes. The Uluyazı Campus is situated on Karlık hill (altitude of 920 m.), different from the alluvial unit (altitude of 725 m.) belonging to the Tatlı and Acı streams that pass through the city centre. The number of blows obtained with SPT was used in this study to evaluate the liquefaction potential of soils (Samireh, 2025). The “Simplified Procedure”, a method developed by Youd & Noble (1997) and based on field data, which is also widely accepted in liquefaction analyses, was used. For HSK-1, SPT-1 (between 1.50 and 1.95 meters) since FS = 5.23 > 1, liquefaction is not expected in the examined soil layer.

3.4. Bearing capacity analysis

In soil bearing capacity calculations, the ultimate bearing capacity (q_f) was determined using the approach proposed by Skempton (1951) and the equation presented by Craig (2004). The safe bearing capacity (q_s) was obtained by dividing the q_f value by the safety factor (GS). The safety factor was selected within the range of 2–5 based on the method proposed by Uzuner & Özmen (1991), and the commonly accepted value of SF = 3 was considered in the calculations. In the ground where the HSK-1 drilling well was opened, the road fill load at 0.00–2.00 m rested on a clay unit with an N value of 36 and PI = 35%.

According to Stroud (1974), based on the Plasticity Index (PI) and undrained shear strength relationship table, PI = 35%. (GS = 3 has been taken due to the presence of residential areas around the Uluyazı Campus Road and the risk of landslides in some places) The maximum stress value reaching the base from the 2.00-meter road fill load is 40 kN/m^2.

Since the safe ultimate bearing capacity value of the road embankment base (120.62 kN/m^2) is greater than the stress value to be transferred (40 kN/m^2) from the road embankment, no bearing capacity problem is expected in the ground where borehole HSK-1 was drilled.

3.5. Soil improvement method

A pile system was implemented as a soil improvement method to address soil and landslide conditions on the campus road of Çankırı Karatekin University (Figure 8). To remedy the structural defects on the road, the collapsed sections were excavated and removed, and soil reinforcement work was carried out to repair the damaged sections.

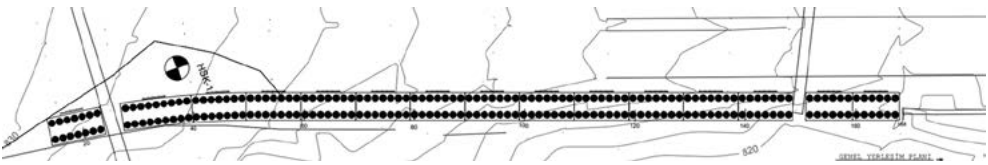

Figure 8. Bored pile application points

The goal is to ensure ground stability with a 2-row, 120 cm diameter, 1.4-meter spaced, 35-meter-long fore pile support structure. A bored pile consists of 3 woven reinforcements, each 12 meters long, joined end to end. Thus, the bored pile machine drove 200 piles to a depth of 35 meters. The bored piles are connected to each other by a top-level cap beam. The size of the cap beam is 1.2 m. Φ32 diameter longitudinal reinforcement (length 12 m); 24 pieces, Φ16 diameter main stirrups; 6 pieces, Φ10 diameter auxiliary stirrups; 97 pieces of 1.5 m reinforcement bars spaced 10 cm apart; in each drilling hole: Φ32 longitudinal reinforcement × 3 = 24 pieces × 3 = 72 pieces; Φ16 main stirrups × 3 = 6 × 3 = 18 pieces; Φ10 auxiliary stirrups × 3 = 97 × 3 = 291 pieces were used. C30/37 class concrete was poured into the holes dug for the piles.

Similarly, in the wells dug for the pile foundation ground improvement application, the first 5 meters consisted of fill gravel, followed by hard clay between 5 and 10 meters, and gypsum-rich claystone and mudstone with low strength between 10 and 35 meters (Figures 9, 10).

Figure 9. (a, b) Drilling work related to bored pile works in the field, (c) Bringing the bored pile reinforcements to the study area

Figure 10. (a) Reinforcement workbench set up in the inspection area; (b, c, d) Preparation of reinforcements with stirrups and steel ties; (e) Circular section drilling for bored pile application; (f) Placement of steel reinforcement in the bored pile hole; (g) Formation of bored piles; (h, i) Application of the bored pile work with two rows; (j, k) Reinforcement and concrete of the cap beam

Conclusion

To determine the ground characteristics and identify the spread of deformations in the landslide area, the relevant company drilled three boreholes, reaching a total depth of 60.00 m. The groundwater level was measured between 5.0 and 6.5 m. In the study area, located approximately 42 km south of the North Anatolian Fault Zone (NAFZ), lithological units were examined at the Uluyazı site. In the study area, gypsum-bearing claystone, mudstone, and fine-grained sandstone belonging to the Bozkır Formation were observed. It was determined that north-south cracks formed in the landslide area, with the direction of movement from northwest to southeast.

Based on both field observations and SPT results, it was understood that the ground in the area where the landslide occurred consisted mainly of clay and silty clay. The landslide was defined as a soil slide. The landslide caused subsidence, cracks, and fissures in the road pavement. It was understood that gypsum blocks taken from the road cutting were used as fill material in the road infrastructure. Melting voids occurred as a result of the interaction of gypsum levels with groundwater and surface water. In addition, the rise/swelling of the clayey soil from the base into the sub-base and base materials also triggered the landslide on the road route. This situation indicates that the clayey structure of the ground is facing not only physical but also chemical dissolution. The shallow groundwater level (5.0–6.5 m) gradually dissolved the gypsiferous material in the fill, creating invisible voids beneath the road. Consequently, the combination of swelling pressure from the clayey soil and these melting voids led to inevitable cracks and settlements in the road superstructure.

Drilling operations were monitored, and corrected blow counts and standardized $N_{1.60}$ values were calculated for soil problems (liquefaction, soil settlement analysis, soil bearing capacity) based on the obtained standard penetration test (SPT) samples. N_{60} values were found to be 10–35 or >35. The soil class in the study area is mostly highly plastic clay (CH), with some areas exhibiting sandy clay (SC) characteristics. Consolidation settlement is expected in all silts and clay soils with medium dense, dense, and very dense characteristics. However, although calculations performed on clayey and clayey silt soils in the study area showed no problems in terms of liquefaction (FS, 5.23) and bearing capacity, soil improvement was carried out to reduce or limit consolidation settlements.

To prevent landslides, it is essential to reduce the drag force that causes masses to move downhill along the slope or to increase the holding force that prevents the movement of masses. In the study area, the relevant institution and company opted for the use of bored piles to transfer the structural loads from weak soils to more stable soils and to ensure highway safety in the event of natural disasters such as landslides, ground movement, and earthquakes. In this context, as part of the landslide solution proposal, two rows of 200 piles, each 120 cm in diameter, spaced 140 cm apart, and 35 m in length, were installed. Additionally, a 1 m thick cap beam was added.

From a highway engineering perspective, slope stability and improved drainage are critical for road safety and longevity. While bored piles and cap beams applied in landslide areas increase the bearing capacity of the soil, the selection of road fill and subbase materials must be optimised in conjunction with the drainage system. In particular, measures such as open drainage channels, horizontal drainage pipes, and slope cover systems should be implemented to remove surface and groundwater from the roadbed. In addition, controlled excavation and grading work along the road, taking into account the mechanical strength of the fill material and the slope angle, will contribute to the long-term preservation of slope stability. Thus, the risks of deformation and settlement for both the road infrastructure and superstructure can be minimised.

In addition, gypsum block material, which is used as road fill material and is prone to melting when it reacts with water, can be replaced with more durable fill material such as andesite or limestone. During road alignment works, the rock debris removed from the excavated road, which is mostly gypsum-based, negatively affects slope stability and drainage conditions. Therefore, rehabilitation works should be carried out by excavating the road alignment area. In summary, the landslide problem in the region stems primarily from the alternating structure of fine-grained clay, silty clay, and sandy clay soils with gypsum layers. Material selection and water management are also influential factors. While the installed piles and beams structurally anchor the road to solid ground, the success of this system depends on diverting water away from the roadbed and replacing the gypsum fill initially used during road construction with durable materials. This holistic approach will extend the road's lifespan and maximise driving safety.

Declarations

Acknowledgements

This study is derived from Aden-gani Robleh Samireh's MSc Thesis. We would like to thank the 15th Regional Directorate of Highways for their support in the field. We are grateful to anonymous reviewers for their constructive comments on the manuscript. We extend our thanks to Atis Zariņš, Managing Editor, BJRBE, for his editorial suggestions and support.

Author contributions

Methodology, ARS and CYG; Formal analysis, CYG and ARS; Investigation, CYG, ES, ARS, BVB and JB; Data curation, CYG and ARS; Writing – original draft preparation, CYG and ES; Writing – review and editing, ES; Supervision, ES; Project administration, ES. All authors have read and agreed to the published version of the manuscript.

Disclosure statement

Authors hereby confirm that they have no competing financial, professional, or personal interests from other parties.

Statement of the Use of Generative AI and AI-assisted Technologies in the Writing Process

None of the artificial intelligence (AI) applications have been used in the content creation and manuscript preparation.

REFERENCES

AFAD. (2019). *Türkiye Deprem Tehlike Haritası ve Parametreleri [Earthquake Hazard Map and Parameters of Türkiye].* Ministry of Interior, Disaster and Emergency Management Presidency, Ankara.

Akıncı, H., Yavuz Özalp, A., Özalp, M., Temuçin Kılıçer, S., Kılıçoğlu, C., & Everan, E. (2014). Bayes olasılık teoremi kullanılarak heyelan duyarlılık haritalarının üretilmesi [Production of Landslide Susceptibility Maps Using Bayesian Probability Theorem]. In *5th Remote Sensing-Gis Symposium (UZAL-CBS 2014),* October 14–17, 2014, Istanbul.

Ateş, Ş., Özata, A., Gülmez, F. K., Osmançelebioğlu, R., Mutlu, G., Özerk, O. C., Yeleser, L., & Üstün, A. B. (2008). Çankırı ili ve kentsel alanların (il-ilçe merkezleri) yerbilim verileri [Geoscience data of Çankırı Province and urban areas (province-district centers)]. MTA Report No. 11098 (unpublished). Ankara.

Avşar, Ö., Akgün, H., & Koçkar, M. K. (2014). Investigation of the failure mechanism and stabilization of a landslide in weathered tuffite, Giresun, northeastern Turkey. *Environmental Earth Sciences, 72*, 3723–3740. https://doi.org/10.1007/s12665-014-3323-5

Clayton, C. R. I. (1993). *Engineering methods for soil and rock classification: A practical guide*. London, UK: E & FN Spon.

Cooper, A. H., & Gutiérrez, F. (2013). Dealing with gypsum karst problems: hazards, environmental issues, and planning. In Shroder, J. F. (Ed.), *Treatise on geomorphology* (pp. 451–462). Elsevier. https://doi.org/10.1016/B978-0-12-374739-6.00106-8

Craig, R. F. (2004). *Craig's soil mechanics.* Spon Press, London and New York.

Cruden, D. M. (1991). A simple definition of a landslide. *Bulletin of the International Association of Engineering Geology, 43*, 27–29. https://doi.org/10.1007/BF02590167

Çankırı Governorship. (2023). Çankırı ili 2023 yılı çevre durum raporu [Çankırı Province 2023 Environmental Status Report]. Çankırı Provincial Directorate of Environment, Urbanization and Climate Change.

ÇEM. (2016). *Heyelanlar*. Ministry of Environment, Urbanization and Climate Change, Türkiye. General Directorate of Combating Desertification and Erosion. Landslides. https://webdosya.csb.gov.tr/db/cem/icerikler/heyelanlar-20211108102144.pdf (accessed on 5 March 2026).

Das, B. M., & Sobhan, K. (2013). *Principles of geotechnical engineering* (8th ed.). Cengage Learning.

Doğan, U. (2002). Subsidence dolines formed by gypsum karstification at the East of Çankırı. *G.U. Journal of Gazi Educational Faculty, 22*(1), 67–82.

Doğan, U., & Yeşilyurt, S. (2019). Gypsum karst landscape in the Sivas Basin. C. Kuzucuoğlu et al. (Eds.), *Landscapes and Landforms of Turkey, World Geomorphological Landscapes*(pp. 197–206). Springer Nature Switzerland AG. https://doi.org/10.1007/978-3-030-03515-0_6

Erginal, A. E., & Bayrakdar, C. (2005). An example to highway-landslides: İnecik Landslide (Tekirdağ). *Journal of Geography, 14*, 43–53.

Gokceoglu, C., & Aksoy, H. (1996). Landslide susceptibility mapping of the slopes in the residual soils of the Mengen region (Turkey) by deterministic stability analyses and image processing techniques. *Engineering Geology, 44*, 147–161. https://doi.org/10.1016/S0013-7952(97)81260-4

Gökkaya, E., & Tunçel, E. (2019). Natural and human-induced subsidence due to gypsum dissolution: a case study from Inandik, Central Anatolia, Turkey. *Journal of Cave and Karst Studies, 81*(4), 221–232. https://doi.org/10.4311/2019ES0105

Gürsoy, H., Orhan Tatar, O., Mesci, B. L., Canbaz, O., Polat, A., & Akpınar, Z. (2024). Anatomy of a landslide: Evaluation of the importance of basic geological investigations as exemplified in the Kuzulu (Koyulhisar – Sivas, Türkiye) Landslide of 17 March 2005. *Geological Bulletin of Turkey*, *67*, 51–70. https://doi.org/10.25288/tjb.1373825

Idriss, I. M. (1995). An update on the Seed–Idriss simplified procedure for evaluating liquefaction potential [H. B. Seed Memorial Lecture]. University of California, Berkeley.

KGM. (2022). *El Kitabı/Handbook*. General Directorate of Highways, Türkiye. https://www.scribd.com/document/743787936/KGM-El-Ki-tabi-2022 (accessed on 5 March 2026).

Ketin, İ. (1976). San Andreas ve Kuzey Anadolu Fayları arasında bir karşılaştırma. *Türkiye Jeoloji Kurumu Bülteni, 19,* 149–154.

Kömüşcü, A. U., Aksoy, M., Çelik, S., Ciba, Ö.F., Uğurlu, A., Turgu, E., & Ünal, E. (2021). 22 Ağustos 2020 Tarihinde Giresun ve İlçelerinde Meydana Gelen Şiddetli Yağış ve Sel Olayının Meteorolojik ve Hidrometeorolojik Analizi [Meteorological and Hydrometeorological Analysis of Severe Rainfall and Associated Flood Occurred in Giresun on 22 August 2020]. *Su Kaynakları*, *6*(1), 1–14. https://izlik.org/JA32HE45PB

Liao, S. S. C., & Whitman, R. V. (1986). Overburden correction factors for SPT in sand. *Journal of Geotechnical Engineering, 112*(3), 373–377. https://doi.org/10.1061/(ASCE)0733-9410(1986)112:3(373)

MTA. (2001). *1/500 000 scale geological map of Turkiye*, The General Directorate of Mineral Research and Exploration, Ankara.

Ocakoğlu, F., Gökçeoğlu, C., & Ercanoğlu, M. (2002). Dynamics of a complex mass movement triggered by heavy rainfall: A case study from NW Turkey. *Geomorphology, 42* (3–4), 329–341. https://doi.org/10.1016/S0169-555X(01)00094-0

Özçelik, A., Yiğit, A. E., Işık, B., Arıtürk, M. A., Özen, Ö., & Büyükurvayli, B. (2016). Determination of karstic cavities and sinkholes by geophysical methods: Inandık Village Application. In İ. Keskin, & C. Göloğlu (Eds.), *Proceedings of International Symposium on Natural Hazards and Hazard Management* (pp. 543–549).

Robertson, P. K., & Wride, C. E. (1998). Evaluating cyclic liquefaction potential using the cone penetration test. *Canadian Geotechnical Journal, 35*(3), 442–459. https://doi.org/10.1139/t98-017

Samireh, A.-G. R. (2025). *Uluyazı (Çankırı) yolundaki heyelan etüdü ve zemin iyileştirme yöntemleri (Landslide Study and Soil Improvement Methods on the Uluyazi Road, Çankırı)* [Master's Thesis, Çankırı Karatekin University, Graduate Education Institute, Department of Civil Engineering], Çankırı.

Sarıfakıoğlu, E., Sevin, M., Esirtgen, E., Bilgiç, T., Duran, S., Parlak, O., Karabalık, N.N., Alemdar, S., Dilek, Y., & Uysal. İ. (2011). *Çankırı–Çorum Havzasını Çevreleyen Ofiyolitik Kayaçların Jeolojisi: Petrojenezi, Tektoniği ve Cevher İçerikleri [Geology of the Ophiolitic Rocks Surrounding the Çankırı–Çorum Basin: Petrogenesis, Tectonics, and Ore Contents]* (Report no. 11449). The General Directorate of Mineral Research and Exploration Ankara (in Turkish, unpublished).

Sarifakioglu, E., Erin, B., Tırın, M., & Sezgin, İ. İ. (2021). Landslides caused by gypsum levels in Çankırı. *4th International Uni-DOKAP Symposium,* Proceedings Book (pp. 98–113). Giresun, Turkiye.

Seed, H. B., & Idriss, I. M. (1971). *Simplified procedure for evaluating soil liquefaction potential* (Report No. EERC 71–10). University of California, Berkeley, Earthquake Engineering Research Center.
https://ntrl.ntis.gov/NTRL/dashboard/searchResults/titleDetail/PB198009.xhtml

Sevin, M., & Uğuz, M. F. (2011). *1:100.000 Ölçekli Türkiye Jeoloji Haritaları Çankırı G32 paftası [1:100,000 Scale Geological Maps of Türkiye, Çankırı G32 sheet].* Publications of the General Directorate of Mineral Research and Exploration, 148 (in Turkish, unpublished).

Skempton, A. W. (1951). The bearing capacity of clays. *Proceedings, Building Research Congress.* London.
https://www.scribd.com/document/471358150/1951-The-bearing-capacity-of-clays-Building-research-congress-pdf

Stroud, M. A. (1974). The standard penetration test in insensitive clays and soft rocks. *Proceedings of the 1st European Symposium on Penetration Testing,* Stockholm, Sweden, 367–375.
https://www.semanticscholar.org/paper/The-standard-penetration-test-in-insensitive-clays-Stroud/5d3b1726376c5d3a5138bf8da6024e0ec1bd89b0

Terzaghi, K. (1950). Mechanism of landslides. In S. Paige (Ed.), *Application of geology to engineering practice.* Geological Society of America.

Terzaghi, K., & Peck, R. B. (1967). *Soil mechanics in engineering practice* (2nd ed.). New York, NY: John Wiley & Sons.

Tırın, M. (2023). *Uluyazı (*Çankırı*) kampüsünde zemin kaynaklı yol bozulmalarında uygulanan yeni metotlar ve kullanılan malzemeler (New Methods and Materials Used in Soil–Related Road Deterioration in the Uluyazı (Çankırı) Campus, Türkiye* [Master's Thesis, Çankırı Karatekin University, Graduate Education Institute, Department of Civil Engineering], Çankırı.

USGS. (2008). *The landslide handbook – A guide to understanding landslides.* United States Geological Survey, Reston, Virginia.

Uzuner, H., & Özmen, H. (1991). *Zemin mekaniği ve temel mühendisliği* (2. baskı). İstanbul: İTÜ Yayınevi.

Varnes, D. J. (1958). Landslide types and processes. *Landslides and Engineering Practice, 24*, 20–47.

Waltham, T. (2002). Gypsum karst near Sivas Turkey. *Cave and Karst Science, 29*(1), 39–44. https://www.researchgate.net/publication/283525275_Gypsum_karst_near_Sivas_Turkey

Yalcin, A., & Bulut, F. (2007). Landslide susceptibility mapping using GIS and digital photogrammetric techniques: a case study from Ardesen (NE-Turkey). *Natural Hazards, 41*, 201–226. https://doi.org/10.1007/s11069-006-9030-0

Yildiz, M. S., & Sarifakioglu, E. (2022). Investigation in terms of soil characteristics of Inandik (Cankiri,Turkiye) sinkholes due to gypsum karstifıcation, *1st International Karatekin Science and Technology Conference,* Cankiri, Turkiye, 244–251.

Youd, T. L., & Noble, S. K. (1997). Liquefaction criteria based on statistical and probabilistic analyses. *Proceedings of the NCEER Workshop on Evaluation of Liquefaction Resistance of Soils*, National Center for Earthquake Engineering Research, 201–205.

Youd, T. L., Idriss, I. M., Andrus, R. D., Arango, I., Castro, G., Christian, J. T., & Stokoe, K. H. (2001). Liquefaction resistance of soils: Summary report from the 1996 NCEER and 1998 NCEER/NSF workshops on evaluation of liquefaction resistance of soils. *Journal of Geotechnical and Geoenvironmental Engineering, 127*(4), 297–313. https://doi.org/10.1061/(ASCE)1090-0241(2001)127:4(297)